Refractivity estimations from an angle-of-arrival spectrum*

Zhao Xiao-Feng(赵小峰)† and Huang Si-Xun(黄思训)

Institute of Meteorology, PLA University of Science & Technology, Nanjing 211101, *China*

(Received 14 August 2010; revised manuscript received 13 September 2010)

This paper addresses the probability of atmospheric refractivity estimation by using field measurements at an array of radio receivers in terms of angle-of-arrival spectrum. Angle-of-arrival spectrum information is simulated by the ray optics model and refractivity is expressed in the presence of an ideal tri-linear profile. The estimation of the refractivity is organized as an optimization problem and a genetic algorithm is used to search for the optimal solution from various trial refractivity profiles. Theoretical analysis demonstrates the feasibility of this method to retrieve the refractivity parameters. Simulation results indicate that this approach has a fair anti-noise ability and its accuracy performance is mainly dependent on the antenna aperture size and its positions.

Keywords: refractivity estimation, angle-of-arrival spectrum, ray optics model, genetic algorithm
PACS: 92.60.Ta, 78.20.Ci, 02.30.Zz **DOI:** 10.1088/1674-1056/20/2/029201

1. Introduction

Near-horizon electromagnetic wave propagation is largely governed by the distribution of the refractive index in the troposphere.[1] Increased information about refractivity enables more precise assessment of the performance of both communication and radar systems. Conventional methods of refractive index measurement that consist of detecting the height dependence of temperature, pressure and humidity performed by radiosondes, microwave refractometers or rocketsondes have some drawbacks, such as being expensive and/or difficult to deploy.[2] Therefore, it is necessary to develop new methods for refractivity detection.

Richter[3] has pointed out that the temporal and spatial variations of radar echoes are related to temporal and spatial variations in the layers of the refractivity profile,[3] which motivates research of atmospheric refractivity estimation from radar clutter returns, i.e., refractivity from clutter (RFC). In the last decade, several RFC methods have been proposed.[4−12] Detailed discussion of these different RFC algorithms can be found in Refs. [9] and [11]. However, instead of using radar clutter returns, Tabrikian and Krolik[13] proposed using point-to-point microwave measurements as a means of estimating refractivity for the purpose of characterizing surface-based ducts by the maximum a posteriori method. Gerstoft *et al.*[14] have used matched-field processing methods for remote sensing of the refractivity structure by using signal strength measurements from a single emitter to an array of radio receivers.

The objective of this paper is to introduce a novel approach for refractivity estimation by using field measurements at an array of radio receivers in terms of the angle-of-arrival (AoA) spectrum. The remainder of this paper is organized as follows. In Section 2, the concept of the AoA spectrum is introduced. Section 3 gives a detailed description of the calculation of the AoA spectrum from the ray optics model. Finally, discussions of simulated runs for refractivity estimation are demonstrated in Section 4.

2. Angle-of-arrival

One of the factors limiting the performance of line-of-sight communication systems is the occurrence of multi-path propagation. Multi-path propagation can be derived from two basic mechanisms, namely ground reflections and atmospheric refractions. Systems devised to reduce the effects of multi-path usually employ some form of diversity. It has been shown that angle diversity can be effective due to separation in the AoA in the vertical plane of individual rays (see Fig. 1).[15] The aim of this section is to provide information relating to the distribution of rays in a multi-path situation in AoA and amplitude.

*Project supported by the National Natural Science Foundation of China (Grant No. 40775023).
†Corresponding author. E-mail: zxf_best@126.com
© 2011 Chinese Physical Society and IOP Publishing Ltd

The employed technique utilizes a vertical wide aperture array in order to sample the received signal over a significant height range. Under atmospheric multi-path conditions, the received signal may be modeled as the sum of a small number of plane waves. For N propagation paths, assuming that these are distributed in the vertical plane, we can obtain the received signal $P_{\rm r}$ at the height z above an arbitrary reference point as[16]

$$P_{\rm r}(z) = \sum_{i=1}^{N} A_i \exp\left[{\rm j}\left(\frac{2\pi z}{\lambda}\sin\theta_i - \delta_i\right)\right], \qquad (1)$$

where λ is the wavelength, A_i and θ_i are the amplitude and AoA of the i-th ray in the vertical plane and δ_i is the phase delay at $z = 0$. The AoA spectrum $R(\xi)$ is given by the Fourier transform of the received signal over a vertical aperture,

$$R(\xi) = \int_{-L/2}^{L/2} P_{\rm r}(z)\exp[-{\rm j}2\pi\xi z]{\rm d}z, \qquad (2)$$

where L is the length of the aperture and ξ is the Fourier transform variable. As we can see from the result of Fourier transform, each term in Eq. (2) contains information about the AoA (represented as a shift in the ξ axis) and the amplitudes of the corresponding rays.

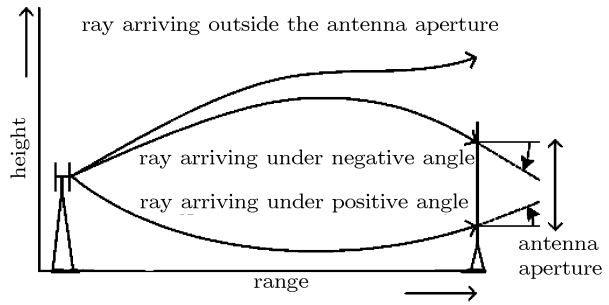


Fig. 1. Geometry of the AoA.

where z is the height in m and $a_{\rm e}$ is the radius of the Earth. The second term in Eq. (3) takes into account the Earth's curvature.

Although the marine atmospheric boundary layer variability that causes microwave ducting is often complex in nature, for the purposes of studying propagation, it is often represented at a given range by bilinear and/or tri-linear height-dependent refractivity profiles.[17] A tri-linear refractivity profile consists of three basic parameters: base height, trapping layer thickness and M-deficit (see Fig. 2). Base height is defined as the height from the surface to the lower boundary of the trapping layer. Thickness is defined as the distance between the lower and the upper boundaries of the trapping layer. The M-deficit is the difference in the modified refractivity values at the two boundaries of the trapping layer. If the value of the base height reduces to zero, the tri-linear profile will become a bilinear profile, which means that the bottom of the duct touches the ground.

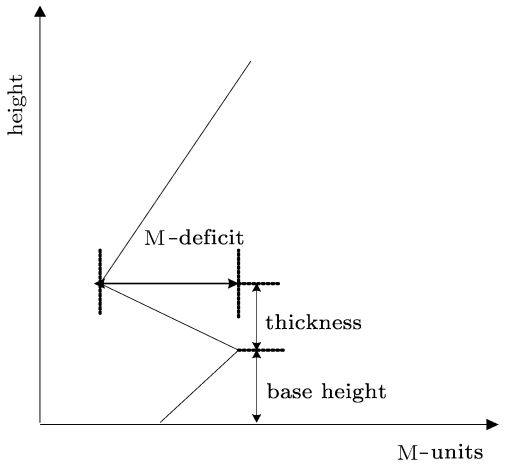


Fig. 2. Parameterization of the refractivity profile.

3. Computation of the AoA from a ray optics model

In this paper, information about the AoA and amplitudes of the corresponding rays are evaluated using a ray optics model.

3.1. Parameterization of refractivity

To describe the refractive conditions, modified refractivity M is preferred to the refractive index n,

$$M = (n-1)\times 10^6 + \frac{z}{a_{\rm e}}, \qquad (3)$$

The tri-linear refractivity profile consists of four height-and-M-unit pairs, which are computed using the following equation:[6]

$$M(z_i) = M_i = M_{i-1} + \left.\frac{{\rm d}M}{{\rm d}z}\right|_i (z_i - z_{i-1}),$$
$$i = 1, 2, 3, \qquad (4)$$

where $z_0 = 0$ is the height at mean sea level, the corresponding M-unit value is $M_0 = 339$ M-units, ${\rm d}M/{\rm d}z|_1 = 0.13$ M-units/m, and ${\rm d}M/{\rm d}z|_3 = 0.118$ M-units/m. In our simulations, the parameters and their search bounds are given in Table 1.

Table 1. Search bounds for tri-linear profile parameters.

parameter	lower bound	upper bound
base height/m	1	700
M-deficit/M-units	1	200
thickness/m	1	200

3.2. Ray optics model

The ray optics method consists of tracing a series of direct and reflected rays through selected control points, and then interpolating the magnitudes of these rays and the phase angles between them at each desired receiver point. The magnitude of each ray is computed from a spreading term relative to free space spreading, and the phase angle is determined from the optical path length differences from the ground range for each ray. The ray trace method is summarized below for a single step.

The elevation angle at the end of the step, α_1, is given by

$$\alpha_1 = \sqrt{\alpha_0^2 + 2 \times 10^{-6}(M_{i+1} - M_i)}, \tag{5}$$

where α_0 is the elevation angle at the beginning of the step, M_i and M_{i+1} represent the modified refractivity at the beginning and end of the step, respectively. The range increment ΔX, spreading increment ΔS and optical path length difference increment ΔD over the step are given as[18]

$$\begin{aligned} \Delta X &= (\alpha_1 - \alpha_0) g_i^{-1}, \\ \Delta S &= (\alpha/\alpha_1 - \alpha/\alpha_0)\, g_i^{-1}, \\ \Delta D &= [(10^{-6} M_i - \alpha_0^2/2)(\alpha_1 - \alpha_0) \\ &\quad + (\alpha_1^3 - \alpha_0^3)/3] g_i^{-1}, \\ g_i &= 10^{-6}(M_{i+1} - M_i)/(z_{i+1} - z_i), \end{aligned} \tag{6}$$

where α is the elevation angle at the transmitter, z_i and z_{i+1} are the heights at the beginning and end of the step, respectively. The total range, X, total spreading term, S, and total optical path length difference, D, are given by the sums of ΔX, ΔS, and ΔD over all steps along each ray. The propagation factors, F_d and F_r, for the direct and reflected rays and the total phase between rays in radians, Ω, are given by

$$\begin{aligned} F_\mathrm{d} &= f_\mathrm{d}^2 \left| X/(\beta_\mathrm{d} S_\mathrm{d}) \right|, \\ F_\mathrm{r} &= f_\mathrm{r}^2 R^2 \left| X/(\beta_\mathrm{r} S_\mathrm{r}) \right|, \\ \Omega &= (D_\mathrm{r} - D_\mathrm{d})k + \phi, \end{aligned} \tag{7}$$

where f_d and f_r are the antenna pattern factors that correspond to the direct and reflected ray elevation angles, respectively, at the transmitter; β_d and β_r are the propagation angles at the receiver point for the direct and reflected rays, respectively; k is the wave number $2\pi/\lambda$, where λ is the wavelength in meters; R and ϕ are the magnitude and phase lag of the Fresnel reflection coefficient.

The propagation factor F of the resultant field between both rays can now be computed by using

$$F^2 = F_\mathrm{d}^2 + F_\mathrm{r}^2 + 2F_\mathrm{d}F_\mathrm{r}\cos\Omega, \tag{8}$$

where F is defined as the ratio of the field strength to the free space field strength. Once F is computed, propagation loss L in dB is determined by

$$L = 20\log f + 20\log X - 10\log F^2 - 27.56, \tag{9}$$

where the base of log is 10, f is the transmitting frequency in MHz.

Now the AoA and amplitudes of the corresponding rays can be computed by Eqs. (5) and (9), respectively. Here, it should be noted that the propagation loss L is used to substitute the receiving amplitude. This simulation has been operated in Refs. [16] and [19]; for detailed discussion of the ray optics model, refer to Ref. [18].

3.3. The AoA simulations

From Eq. (2), we clearly see that the AoA spectrum can be obtained from measured values of amplitude and AoA at the elements of the vertical antenna array. The numerical values of AoA and paths of individual rays for the given atmospheric profile are shown in Fig. 3. Here, the transmitting antenna pattern used in our calculations is a Gaussian antenna pattern. It is designated that the antenna is set at a height of 15 m and operates at a frequency of 10 GHz. The receiver is a 10-element vertical antenna array aperture extending from 11 m to 20 m.

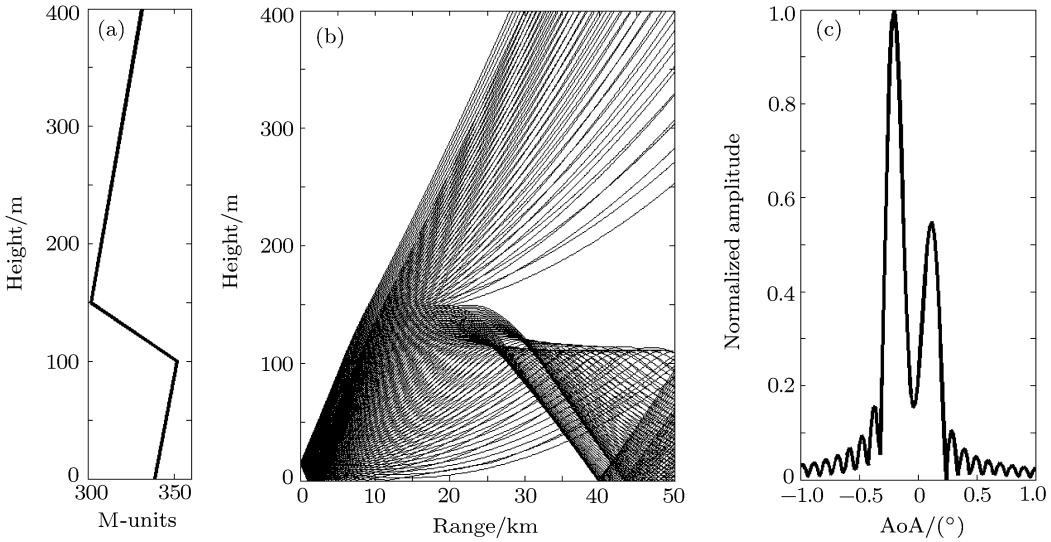


Fig. 3. (a) Refractivity profile with base height 100 m, thickness 50 m and M-deficit 50 M-units: (b) Ray paths in the presence of surface-based duct. (c) The AoA spectrum derived from ray optics model.

4. Refractivity estimation

When the AoA spectrum is measured at a vertical antenna array from a distant transmitter, the received field will depend in some way on the refractive index distribution of the atmosphere. The effect of the height dependence of the refractive index is then registered at the receiving array in terms of either amplitude or AoA at each element of the array.[16]

Since the measured data were not available, numerical simulations were performed. Figure 4 shows simulated AoA spectra with different refractivity profiles. It can be seen that the distribution of the AoA spectrum relies on the atmospheric environment, which indicates that measurement of the AoA spectrum in specific atmospheres might be employed as useful information for estimating atmospheric refractivity.

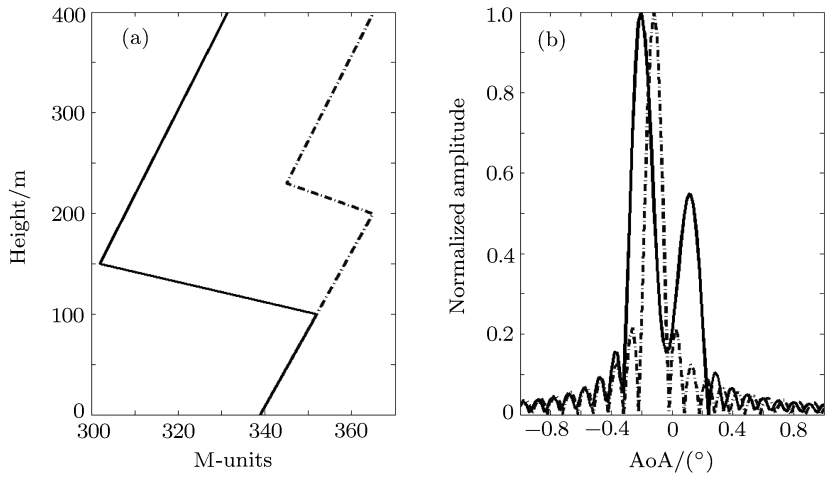


Fig. 4. The AoA spectra according to different refractivity profiles.

The principle of refractivity estimation from the AoA spectrum can be summarized as following two steps.

Step 1 Giving a refractivity profile as the true atmospheric environment, from which the ray optics model is adopted to simulate the AoA spectrum as the spectrum measurements at the receiving antenna array.

Step 2 Perform a set of propagation simulations under various refractivity profiles until a profile is found which gives the best agreement of measured values.

This is an optimization problem to which techniques of evolutionary algorithms can be applied. Here, we use the genetic algorithm (GA).[11,20] The GA is a probabilistic method that searches the domain of all possible solutions. Solutions with a better objective function value are preferred in the course of the algorithm and the whole procedure converges to the optimal solution.

The objective function used here desribes the distance between the given (measured) AoA spectrum and the AoA spectrum of a trial solution,

$$\varphi(\boldsymbol{M}) = \sum_i [R_{\rm m}(\boldsymbol{M}, \xi_i) - R_{\rm s}(\boldsymbol{M}, \xi_i)]^2, \qquad (10)$$

where $\varphi(\boldsymbol{M})$ is the objective function of a trial solution given by modified refractivity vector $\boldsymbol{M}$. The $R_{\rm m}$ and $R_{\rm s}$ are measured and simulated normalized angular dependencies of the AoA spectrum.

In the following, two experiments were performed. In each experiment, the transmitter was given as described in Subsection 3.3. The horizontal distance between the transmitter and the receiver array was 50 km (This is consistent with the real data measurements in Ref. [16]). The GA search parameters are set as: parameter quantization 1024; population size 100; reproduction size 0.2; crossover probability 0.5; jump mutation probability 0.05; creep mutation size 0.16; maximum generation 200.

Experiment 1 The refractivity parameters were given as base height 100 m, thickness 50 m and M-deficit 50 M-units. The receiver antenna array has 10 elements and its aperture size is 9 m. Here, receivers were placed in three different positions, respectively, from 11 m to 20 m, from 31 m to 40 m and both of the two cases. The detailed refractivity parameter values retrieved by GA in terms of the AoA spectrum are given in Table 2.

Table 2. Inversion results from different receiver positions.

	base height/m	thickness/m	M-deficit/M-units	average error/%
true value	100	50	50	—
11 m to 20 m	89.7	45.2	46.4	9.0
31 m to 40 m	92.1	42.1	60.5	14.9
11 m to 20 m 31 m to 40 m	95.0	47.5	56.3	7.5

From Table 2 we can see that although the inversion results from the AoA spectrum are not accurate, they are believable. Different receiver array positions could bring about different inversion values. The results from the two antenna arrays respectively from 11 m to 20 m and 31 m to 40 m are better than the single antenna array. This is because the case of the two antenna arrays is identical to extending the aperture size of the antenna, which could receive more information from the transmitter.

Experiment 2 The refractivity parameters were given as those in experiment 1. Two receiver antenna arrays were placed from 11 m to 20 m and from 31 m to 40 m. In order to test the anti-noise ability of this approach, some Gaussian noise was added to the field measurements to simulate the observing noise.

Table 3. Inversion results with different Gaussian noises.

	base height/m	thickness/m	M-deficit/M-units	average error/%
true Value	100	50	50	—
5% Gaussian noise	96.2	41.3	45.9	9.8
10% Gaussian noise	114.7	46.1	63.5	16.5
20% Gaussian noise	152.3	33.0	55.6	32.5

From Table 3 it is clearly seen that the approach of refractivity estimation from the AoA spectrum by GA has fair anti-noise ability. It is reasonable that the inversion accuracy decreases with the increment of the noise. When the Gaussian noise is only 5%, the results are good enough. In a 10% Gaussian noise case, the inversion results are acceptable. However, in a 20% Gaussian noise case, although the retrieved M-

deficit value is good, the base height value has made the whole inversion meaningless.

5. Conclusion

The principle refractivity profile remote sensing in terms of the AoA spectrum by GA was introduced. Since measured data were not available, a simulated AoA spectrum was used. Results were presented to show that the performance of the estimation is dependent on the tri-linear refractivity profile model. It was shown that reasonable estimation results could be expected for profile with this method. The inversion accuracy is dependent on the antenna aperture size and its positions.

In our estimations, the AoA spectrum information was calculated by the ray optics model. Dockery has pointed out that, in microwave propagation simulation, the ray optics model is not as accurate enough as the parabolic equation model and is supported only over water, low antenna-height applications.[21] However, in comparison to the parabolic equation model, the ray optics model requires less computation time. Our future work will be mainly focused on applying the parabolic equation model to simulate the AoA spectrum and performing real measured data inversions.

References

[1] Yan H J, Fu Y and Hong Z J 2006 *Introduction to Modern Atmospheric Refraction* (Shanghai: Shanghai Science and Educational Press) (in Chinese)

[2] Halvey R A 1983 *Proc. IEEE* Part F **130** 643

[3] Richter J H 1969 *Radio Sci.* **4** 1261

[4] Rogers L T 2000 *Radio Sci.* **35** 955

[5] Gerstoft P, Rogers L T, Krolik J L and Hodgkiss W S 2003 *Radio Sci.* **38** 8053

[6] Barrios A E 2004 *Radio Sci.* **39** RS6013 doi:10.1029/2003RS002930

[7] Weckwerth T M, Petter C R, Fabry F, Park S, Lemone M A and Wilson J W 2005 *J. Appl. Meteor.* **44** 285

[8] Yardim C, Gerstoft P and Hodgkiss W S 2006 *IEEE Trans. Antennas Propag.* **54** 1318

[9] Vasudevan S, Anderson R H, Kraut S, Gerstoft P, Rogers L T and Krolik J 2007 *Radio Sci.* **42** RS2014 doi:10.1029/2005RS003423

[10] Wang B, Wu Z S, Zhao Z W and Wang H G 2009 *Prog. Electromagn. Res.* M **9** 79

[11] Huang S X, Zhao X F and Sheng Z 2009 *Chin. Phys.* B **18** 5084

[12] Zhao X F, Huang S X and Sheng Z 2010 *Chin. Phys.* B **19** 049201

[13] Tabrikian J and Krolik J L 1999 *IEEE Trans. Antennas Propag.* **47** 1727

[14] Gerstoft P, Gingras D F, Rogers L T and Hodgkiss W S 2000 *IEEE Trans. Antennas Propag.* **48** 345

[15] Webster A R and Merritt T S 1990 *IEEE Trans. Commun.* **38** 25

[16] Akbarpour R and Webster A R 2005 *IEEE Trans. Antennas Propag.* **53** 3785

[17] Rogers L T 1996 *IEEE Trans. Antennas Propag.* **44** 460

[18] Barrios A E 2003 *Considerations in the Development of the Advanced Propagation Model (APM) for U.S. Navy Applications* AD-A **445** 237

[19] Valtr P and Pechac P 2005 *Radioengieering* **14** 98

[20] Yang G, Reinstein L E, Pai S, Xu Z and Carroll D L 1998 *Medical Physics* **25** 2308

[21] Dockery G D 1998 *Johns Hopkins APL Technical Digest* **19** 283